# Control/structure optimization approach for minimum-time reconfiguration of tensegrity systems

J.B. Aldrich[a], R.E. Skelton[a]

[a]Dept. of Mechanical and Aerospace Engineering, Univ. of Cal., La Jolla, CA 92093–0411

## ABSTRACT

For a new class of tendon-driven robotic systems that is generalized to include tensegrity structures, this paper focuses on a method to jointly optimize the control law and the structural complexity for a given point-to-point maneuvering task. By fixing external geometry, the number of identical stages within the domain is varied until a minimal mass design is achieved. For the deployment phase, a new method is introduced which determines the tendon force inputs from a set of admissible, non-saturating inputs, that will reconfigure each kinematically invertible unit along its own path in minimum time. The approach utilizes the existence conditions and solution of a linear algebra problem that describe how the set of admissible tendon forces is mapped onto the set of path-dependent torques. Since this mapping is not one-to-one, free parameters in the control law always exist. An infinity-norm minimization with respect to these free parameters is responsible for saturation avoidance. In addition to the required time to deploy, the expended control energy during the post-movement phase is also minimized with respect to the total number of stages. Conditions under which these independent minimizations yield the same robot illustrate the importance of considering control/structure interaction within this new robotics paradigm.

## 1. INTRODUCTION

Robotic automation of repetitive assembly processes continues to gain more acceptance as an effective means to reduce labor costs and increase productivity in many manufacturing industries. This is especially true in pick-and-place applications where the objective is to move from one position to another quickly and accurately. As a result of driving the trajectories faster and faster, the inertial dynamics of typical robots become too large to be ignored, and therefore must be compensated by a feedback controller. Assuming that a sufficiently accurate plant model is available, the standard approach to this control problem is to implement a feedback-linearizing computed-torque controller for the reconfiguration phase [1–3], followed by a linear controller for the post-movement phase. *Theoretically*, this approach allows arbitrarily large configuration changes within the robot's workspace to occur quickly. As a practical matter, however, reconfiguration in near-zero time is not possible since the inertial forces to be carried by the actuators would have excessive magnitude causing actuator saturation. One way to circumvent this problem is to make the robot lose weight. For instance, a lighter design is possible by placing the heavy actuators at the base of the manipulator where a pulley-tendon system transmits torque remotely [4], Fig. (1a,b). Unfortunately, tendon compliance makes it difficult to transmit torque with sufficient bandwidth [5]. One approach that circumvents this problem is to design a mechanism that reduces tendon usage [6]. Alternatively, bandwidth can also be recovered by reducing system mass [7]. For instance, the tensegrity systems in Fig. (1c–h) can be designed with exceptionally low system mass and superior saturation avoidance capability since large bending moments normally present in the links get absorbed in the tendon network [8]. The work herein suggests that tensegrity concepts will revolutionize the manner in which tendon-driven systems are designed, controlled and utilized. We believe this will become especially true in environments where agile maneuvering and delicate object handling require a "soft" touch.

In the sections that follow, we address the following questions: Given a set of admissible tendon forces, how should the control law be designed? For a given robot, which tendon network sustains more torque? What is its minimum-time trajectory along a prescribed path? How can feedback be used to keep it on track? Lastly, can the control law and structure be jointly optimized for a given point-to-point maneuvering task?

---

For further author information send correspondence to J.B.A.: e-mail: jaldrich@ucsd.edu, telephone: 1 858 822 2020.
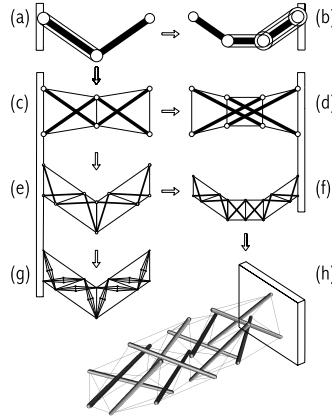
**Figure 1**. Proposed tensegrity robot evolution

## 2. ADMISSIBLE TENDON FORCES

A necessary condition for a tendon-driven robotic system is that all tendons be taut and unbroken. When this condition holds, we say that the tendon actuation system is in a state of unsaturation as follows.

**Definition 1.** An $m$-tendon actuation system is said to be *unsaturated* if $t \in \mathcal{A}$ where

$$\mathcal{A} := \{t \in R^m : 0 < t_i < f_{yi}, \}$$

and $t_i$ is the tension in the $i^{th}$ tendon, and $f_{yi}$ is the yield force (max allowable tension) for the $i^{th}$ tendon. A system that is not *unsaturated*, is *saturated*. Set $\mathcal{A}$ is the set of *admissible* tendon forces.

## 3. CONTROL PROBLEM STATEMENT

Given a desired reference trajectory, $q_d$, for a tendon-driven rigid-body system modelled as

$$M(q)\ddot{q} + V(q, \dot{q})\dot{q} + g(q) = G(q)t$$

($q \in R^n$, $t \in \mathcal{A} \subset R^m$, $M$ is square), we seek to answer the question: Does there exist admissible tendon forces $t$ to yield the following closed loop system?

$$\ddot{z} + K_v \dot{z} + K_p z + K_i v = 0$$
$$z = q - q_d = \dot{v}$$

Yes, if and only if there exists $t \in \mathcal{A}$ to solve

$$Gt = M(\ddot{q}_d - K_v \dot{z} - K_p z - K_i \nu) + V\dot{q} + g = \tau. \tag{1}$$

There exists a $t \in R^m$ solving (1) iff $G_L \tau = 0$ where $G_L G = 0$ and $G_L G_L^T \succ 0$. If $t \in R^m$ exists to solve (1), then all solutions are given by

$$t = G^+ \tau + G_R \eta \tag{2}$$

where $GG_R = 0$ and $G_R^T G_R \succ 0$.

It is important to recognize two facts. First, the dimension of the nullspace of $G$ is $\rho(G) = m - \text{rank}(G)$. Hence, $\eta$ contains $\rho(G)$ free parameters that have neither been characterized nor optimized by the robotics community [9–12]. Second, even if a solution $t \in R^m$ exists there is no guarantee that there exists a choice for $\eta$ such that $t \in \mathcal{A}$. An approach that resolves these facts is the main contribution of this paper and [12].

# 4. HOW SHOULD FREE PARAMETERS BE OPTIMIZED?

In order to understand how to optimize the free parameters $\eta$, a more suitable saturation definition is helpful. Toward this end, we define $D = \mathrm{diag} \begin{bmatrix} 2/f_{y1} & 2/f_{y2} & \cdots & 2/f_{ym} \end{bmatrix}$, $e = \begin{bmatrix} 1 & \cdots & 1 \end{bmatrix}^T$ and $t = \begin{bmatrix} t_1 & \cdots & t_m \end{bmatrix}^T$ and establish a series of equivalent statements as follows. (A proof of the theorem 1 is given in [12].)

**Theorem 1.** The following statements are equivalent:

   (i) The $m$-tendon actuation system is *unsaturated*.

   (ii) There exists a $\delta < 1$ such that $\|Dt - e\|_\infty \leq \delta$.

   (iii) $t + d \in \mathcal{A}$ if $\|d\|_\infty < (1 - \delta) \min_i f_{yi}/2$.

**Corollary 1.** If the tendons are uniform, i.e. $f_{yi} = f_y$ for $i = 1\!:\!m$, then
$D^{-1}e = (f_y/2)e =: t_d$ and the following statements are equivalent:

   (i) The $m$-tendon actuation system is *unsaturated*.

   (ii) $\gamma := f_y/2 - \|t - t_d\|_\infty > 0$

   (iii) $t + d \in \mathcal{A}$ if and only if $\|d\|_\infty < \gamma$

In order to keep a tendon actuation system in a state of unsaturation that is robust to perturbations, $d$, we look to part (iii) of the corollary to motivate the following robust control objective.

**Robust control objective:** Maximize saturation margin, $\gamma$, w.r.t. free parameters in real-time [12].

An equivalent objective follows immediately from part $(ii)$ of the corollary: Minimize tendon force deviation from $t_d$ (50%-yield) w.r.t. free parameters in real-time,

$$
\begin{aligned}
\eta_\infty^* \quad &:= \quad \arg\min_\eta \|t(\eta) - t_d\|_\infty \\
&= \quad \arg\min_{\theta, \eta} \ \theta \quad \text{s.t.} \quad \theta \geq 0, \quad -\theta e \leq G^\perp \eta + G^+ \tau - t_d \leq \theta e
\end{aligned}
$$

where $t(\eta)$ is defined by (2) with the $G^\perp$ notation replacing $G_R$ hereafter. Notice the *min-max minimizer*, $\eta_\infty^*$, requires a real-time linear program solution. Alternatively, the *least-squares minimizer*, $\eta_2^*$, can be expressed analytically, and computed independent of the controller as follows

$$
\eta_2^* \quad := \quad \arg\min_\eta \|t(\eta) - t_d\|_2 = \arg\min_\eta \|G^\perp \eta + G^+ \tau - t_d\|_2 = G^{\perp T} t_d
$$

where $G^\perp G^{\perp T} t_d$ is the orthonormal projection of $t_d$ onto null$(G)$. The tradeoff is that $\eta_2^*$ is slightly less effective than $\eta_\infty^*$ for saturation avoidance. In both cases, however, if the applied loading, $\tau$, is sufficiently large, then the axial force in at least one tendon will no longer be admissible, i.e. $t(\eta_p^*) \notin \mathcal{A}$ for $p = 2, \infty$. This problem can be circumvented by increasing tendon strength, $f_y$, until $t(\eta_p^*) \in \mathcal{A}$. Alternatively, the free parameters can be chosen so as to minimize the maximum tendon force subject to a tautness constraint, $t > 0$. That is,

$$
\begin{aligned}
\eta_\infty^\dagger \quad &:= \quad \arg\min_\eta \|t(\eta)\|_\infty \quad \text{s.t.} \quad t_i \geq \underline{t} > 0 \ \ \forall i \\
&= \quad \arg\min_{\bar{t}, \eta} \ \bar{t} \quad \text{s.t.} \quad \bar{t} \geq \underline{t} > 0, \quad \underline{t}e \leq G^\perp \eta + G^+ \tau \leq \bar{t}e \\
\eta_2^\dagger \quad &:= \quad \arg\min_\eta \|t(\eta)\|_2 \quad \text{s.t.} \quad t_i \geq \underline{t} > 0 \ \ \forall i \\
&= \quad \arg\min_\eta \ \eta^T \eta \quad \text{s.t.} \quad \underline{t}e \leq G^\perp \eta + G^+ \tau
\end{aligned}
$$

Notice the *constrained least-squares minimizer*, $\eta_2^\dagger$, requires a quadratic program, but has only one inequality constraint per tendon. In contrast, the *constrained min-max minimizer*, $\eta_\infty^\dagger$, requires a linear program, but must satisfy two inequality constraints per tendon plus one more. When computation time is not an issue, the

constrained minimizers work best in ultralite applications such as delicate-object handling where minimum force control is desired to give the robot a "soft touch".

**How effective is $\eta_\infty^*$ at saturation avoidance?** For a given torque loading, $\tau$, and robot geometry, $q$, the percent saturation, $S$, can be computed as a function of the free parameters, $\eta$, as

$$S(\eta) := (2/f_y)\|G^\perp(q)\eta + G^+(q)\tau - t_d\|_\infty \tag{3}$$

In the example below, we illustrate how effective $\eta_\infty^*$ is at saturation avoidance in the presence of torque loading and a variable structure geometry.

**Example.** In Fig. (2) we are given two tendon actuation systems for a single link manipulator. The
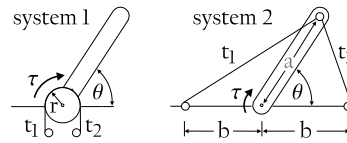


**Figure 2**. Benchmark comparison.

coupling matrices that map $t \in R^2$ into $\tau \in R^1$ are given by $G_1 = r[\begin{array}{cc} 1 & -1 \end{array}]$ for systems 1 and $G_2 = a[\begin{array}{cc} -c_1^{-1/2}e\sin\theta & c_2^{-1/2}e\sin\theta \end{array}]$ for system 2, where $c_1 = 1 + e^2 + 2e\cos\theta$, $c_2 = c_1 - 4e\cos\theta$ and $e = b/a$. We let $a = \sqrt{3}/2$, $b = 1/2$, $r = 1/10$, and plot in Fig. (3) the level curves of percent saturation, $S(\eta_p^*)$, where $\eta_p^*$ is a function of $\tau$ and $\theta$. Fig. (3b,c) shows the least-squares minimizer is slightly inferior to the minmax minimizer
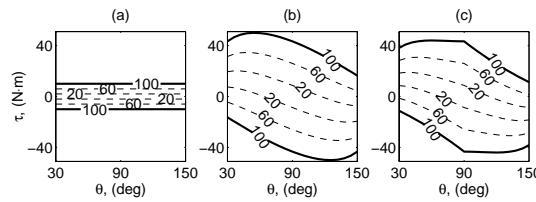


**Figure 3.** Level curves of percent saturation, $S(\eta_p^*)$, as a function of torque and geometry, $\tau$ and $\theta$. (a) system 1 with $p = \infty$, (b) system 2 with $p = \infty$, (c) system 2 with $p = 2$.

for saturation avoidance. Fig. (3a,b) shows that system two is guaranteed to sustain greater torque than system one. The apparent *leverage advantage* of system two extends to most tensegrity systems [12]. Increasing the sustainable torque means point-to-point maneuvering can occur in less time.

## 5. MIN-TIME CONTROL OF MULTI-CELL MULTI-PATH (MCMP) SYSTEMS

In [12], we posed the question: What admissible tendon force inputs will move a kinematically-invertable plant from point A to point B along a prescribed path in minimum time? In this section, we consider MCMP systems—a class of robotic tensegrity structures that are not kinematically-invertable, but can be partitioned into *independent* kinematically-invertible units, or "cells". In MCMP, every link in the robot belongs to one and only one cell, and each cell's configuration can be assigned independently of the other cells' configurations.

*Problem Statement: For a given MCMP system, what admissible tendon force inputs will simultaneously reconfigure each cell along its own path in minimum time?*

As before, the solution is broken down into four tasks: First, is *path-construction*. Second, convert the free dynamics to *path-following dynamics*. Third, substitute path-following dynamics into tendon saturation constraint to get a *path-acceleration constraint*. Fourth, construct the *minimum-time solution* by maximizing path velocity at each point on path [13].

**Path-construction.** For the MCMP class of robotic tensegrity structures each cell's tip-to-tip configuration vector can be written as an explicit function of its joint angles, $q$, or the distance along the path, $s$, as follows

$$r(q) := \begin{bmatrix} r_1(q_1) \\ r_2(q_2) \\ \vdots \\ r_m(q_m) \end{bmatrix} = \begin{bmatrix} \tilde{r}_1(s) \\ \tilde{r}_2(s) \\ \vdots \\ \tilde{r}_m(s) \end{bmatrix} =: \tilde{r}(s) \tag{4}$$

It is easy to determine $r(q)$ from the forward kinematics. To illustrate how $\tilde{r}(s)$ can be constructed, consider as an example the definition of a differentiable tubular surface of radius $\gamma(s)$ around curve $\alpha(s)$ [14],

$$\begin{aligned} x(s,v) = & \quad \alpha(s) + \gamma(s)\left[n\cos v + b\sin v\right], \quad s \in I, \quad v \in [0, 2\pi] \\ & n = \alpha''(s)/|\alpha''(s)| \\ & b = \alpha'(s) \times n \end{aligned}$$

where $\alpha : I \rightarrow R^3$ is any differentiable curve with nonzero slope and curvature everywhere parameterized by arclength $s$. $n$ and $b$ are the normal and binormal vectors of $\alpha$, respectively. As we shall see, this tube parameterization can be used to define deployment paths for each stage or for the multi-stage tensegrity system as a whole. For a tensegrity structure with $m$ bars per stage, and $n$ stages, we expand equation (4) as

$$r_i(q_i) := \begin{bmatrix} r_{i1}(q_{i1}) \\ r_{i2}(q_{i2}) \\ \vdots \\ r_{in}(q_{in}) \end{bmatrix} = \begin{bmatrix} \tilde{r}_{i1}(s) \\ \tilde{r}_{i2}(s) \\ \vdots \\ \tilde{r}_{in}(s) \end{bmatrix} =: \tilde{r}_i(s)$$

where $i=1{:}m$. Now it is possible to compute all tip-to-tip configuration vectors for each cell as a function of a single parameter that keeps the tips on the surface as follows

$$\tilde{r}_{ij}(s) = x(s_j, v_i) - x(s_{j-1}, v_i)$$

where $i=1{:}m$ and $j=1{:}n$. Hence, the robot designer is free to choose both the curve and radius of the tubular surface. For instance, suppose we are interested in a point-to-point maneuver where the tips of each cell are prescribed to stay on a tubular surface centered about a helix whose curve, normal and binormal vectors are:

$$\alpha(s_j) = \begin{bmatrix} a\cos(s_j/c) - a \\ a\sin(s_j/c) \\ bs_j/c \end{bmatrix}, \qquad n(s_j) = \begin{bmatrix} -\cos(s_j/c) \\ -\sin(s_j/c) \\ 0 \end{bmatrix}, \qquad b(s_j) = \begin{bmatrix} (b/c)\sin(s_j/c) \\ (b/c)\cos(s_j/c) \\ a/c \end{bmatrix}$$

where $s_j = s\frac{j}{n}$ and $v_i = \frac{2i\pi}{m}$. The deployed configuration of the robot is pictured in Fig. (4).

**Path-following dynamics.** Differentiating (4) w.r.t. time twice yields $r_q\dot{q} = \tilde{r}_s\dot{s}$ and $r_q\ddot{q} + \dot{r}_q\dot{q} = \tilde{r}_s\ddot{s} + \tilde{r}_{ss}\dot{s}^2$ where $r_q = \partial r/\partial q$ is the Jacobian,

$$r_q = \begin{bmatrix} \frac{\partial r_1}{\partial q_1} & & \\ & \ddots & \\ & & \frac{\partial r_m}{\partial q_m} \end{bmatrix}, \qquad \dot{r}_q = \begin{bmatrix} \frac{\partial}{\partial t}\frac{\partial r_1}{\partial q_1} & & \\ & \ddots & \\ & & \frac{\partial}{\partial t}\frac{\partial r_m}{\partial q_m} \end{bmatrix}, \qquad \tilde{r}_s = \begin{bmatrix} \frac{\partial \tilde{r}_1}{\partial s} \\ \vdots \\ \frac{\partial \tilde{r}_m}{\partial s} \end{bmatrix}, \qquad \tilde{r}_{ss} = \begin{bmatrix} \frac{\partial^2 \tilde{r}_1}{\partial s^2} \\ \vdots \\ \frac{\partial^2 \tilde{r}_m}{\partial s^2} \end{bmatrix}$$

Notice that our choice of local coordinates for each cell yields a block diagonal Jacobian. In contrast, if we had defined $r$ and $\tilde{r}$ with respect to a fixed reference frame, the Jacobian would be block lower triangular. We now can compute $q = q(s)$, $\dot{q} = \dot{q}(s, \dot{s})$, $\ddot{q} = \ddot{q}(s, \dot{s}, \ddot{s})$. Hence, the free dynamics, $M(q)\ddot{q} + h(q, \dot{q}) = \tau$ can now be converted to the *path-following dynamics*:

$$\tau(s, \dot{s}, \ddot{s}) = u(s)\ddot{s} + v(s, \dot{s})$$
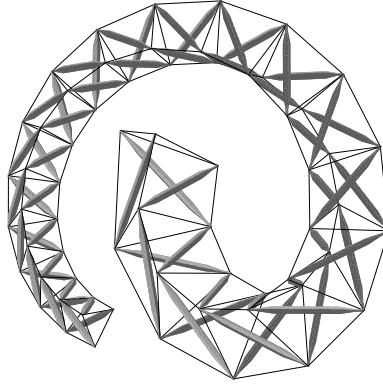
**Figure 4**. Deployed tubular tensegrity structure.

where $u(s) := M(q)r_q^{-1}\tilde{r}_s$ and $v(s, \dot{s}) := M(q)r_q^{-1}(\tilde{r}_{ss}\dot{s}^2 - \dot{r}_q\dot{q}) + h(q, \dot{q})$.

**Path-acceleration constraint.** Recall the linear algebra problem: $\tau(s, \dot{s}, \ddot{s}) = G(s)t$ whose solution $t = G^+\tau + G^\perp\eta$ exists iff $[I - GG^+]\tau = 0$. Assuming solution exists (which is true automatically when $G$ is full row rank), substitute it into the tendon saturation constraint of theorem 1, $\|Dt - e\|_\infty \leq \delta$, to get $-\delta \leq a_i(s, \dot{s}, \eta) + \ddot{s}c_i(s) \leq \delta$ for $i = 1$ to $m$, where $a = DG^\perp\eta + DG^+v - e$ and $c = DG^+u$. Rearrangement yields *path-acceleration constraint*,

$$f(s, \dot{s}, \eta) \leq \ddot{s} \leq g(s, \dot{s}, \eta)$$

where $f(s, \dot{s}, \eta) = \max_i ((-\text{sign}(c_i)\delta - a_i)/c_i)$ and $g(s, \dot{s}, \eta) = \min_i ((\text{sign}(c_i)\delta - a_i)/c_i)$.

**Minimum-time solution.** The minimum-time solution is obtained by choosing the acceleration $\ddot{s}$ to make the velocity $\dot{s}$ as large as possible at every point $s$ without violating $f(s, \dot{s}, \eta) \leq g(s, \dot{s}, \eta)$. This follows by minimizing the cost,

$$J = \int_0^T dt = \int_A^B \frac{1}{\dot{s}(s)} ds$$

In [13], it was shown that $J$ is minimized if and only if $\ddot{s}$ always takes either its largest or its smallest admissible value. In summary, it is easy to show the following.

**Theorem 2.** The path-following minimum time solution subject to $t \in \mathcal{A}$ is obtained by switching between maximum acceleration, $\ddot{s} = g(s, \dot{s}, \eta_\infty^*)$, and maximum deceleration $\ddot{s} = f(s, \dot{s}, \eta_\infty^*)$ where $\eta_\infty^* = arg\min_\eta \|A(s)\eta + b(s, \dot{s}) + \ddot{s}c(s)\|_\infty$ and $A = DG^\perp$, $b = DG^+v - e$, $c = DG^+u$.

**Corollary 2.** The path-following minimum time solution subject to $t \in \mathcal{A}$ and $\min_\eta \|Dt(\eta) - e\|_2$ is obtained by switching between $\ddot{s} = g(s, \dot{s}, \eta_2^*)$ and $\ddot{s} = f(s, \dot{s}, \eta_2^*)$ where $\eta_2^* = G^{\perp T}(s)D^{-1}e$.

The remaining task is to determine when to switch between $f$ and $g$. Techniques for locating switching points are described in [13,15] and applied to an example in [12]. The minimum time solution yields the desired open-loop trajectory, $q_d$. Feedback can be used to reduce the tracking error, $z = q - q_d$, as discussed next.

## 6. PATH-TRACKING CONTROL WITH MODEL UNCERTAINTY COMPENSATION

For the uncertain plant, $M(q)\ddot{q} + V(q, \dot{q})\dot{q} + g(q) + d_w = G\hat{t}$, we computed $\hat{t} = \hat{G}^\perp\eta + \hat{G}^+\hat{\tau} + u_r$ in [12] as the feedback law where $u_r$ is a robust control input to be designed, $d_w$ is an external disturbance and we assume

$G = G(q)$. Three sources of parametric uncertainty are considered here, namely, the *standard error*, $\tilde{\tau} = \tau - \hat{\tau}$, that occurs in all robotic systems, and two tensegrity-based errors,

$$
\begin{aligned}
\tilde{G}^+ &= G^+ - \hat{G}^+ \quad \text{psuedoinverse error} \\
\tilde{G}^\perp &= G^\perp - \hat{G}^\perp \quad \text{nullspace error}
\end{aligned}
$$

Assuming $q$ is measured exactly and $G$ is full row rank, the closed loop system becomes $M(q)\ddot{q} + V(q,\dot{q})\dot{q} + g(q) + d_t = \tau + G u_r$, where the total disturbance is $d_t = d_w + G\tilde{G}^+ \tau + G\tilde{G}^\perp \eta + G\hat{G}^+ \tilde{\tau}$.

**Lyapunov design.** Given time-optimal reference trajectories how do we stay on path using feedback? This can be solved by using a Lyapunov function: $V_1 = \frac{1}{2} r^T M(q) r$ where $r = \Lambda z + \dot{z}$. Then we choose nominal input as $\tau = -Y(\cdot)\phi - K_r r$ with error $\tilde{\tau} = -Y(\cdot)\tilde{\phi}$. The robust input, $u_r = k_d \hat{G}^+ \operatorname{sgn}(r)$ can be implemented without error since we assume the state is known exactly. The psuedoinverse error is bounded as $-\bar{g}I \leq G\tilde{G}^+ \leq \bar{g}I$, where $0 \leq \bar{g} \leq 1$. In [12], we show the time-derivative of the Lyapunov function becomes negative semi-definite, i.e. $\dot{V}_1 \leq -r^T K_r r$, if the robust control gain is sufficiently large and negative compared to external disturbances and those introduced by the tensegrity paradigm, That is, $k_d < 0$, and

$$
|k_d| \geq \frac{||d_w + G\tilde{G}^+ \tau + G\tilde{G}^\perp \eta + G\hat{G}^+ \tilde{\tau}||_\infty}{(1 - \bar{g})} \tag{5}
$$

If this gain requirement holds, then $\dot{V}_1 \leq 0$ and a La Salle's argument given in [3] can be used to show that the tracking errors are asymptotically stable. The gain requirement on $|k_d|$ can be reduced with the adaptive inertial-related control [3]. Finite-bandwidth robust control is possible by replacing the sign function with a saturation function in $u_r$ [16]. For standard non-tensegrity robots, (5) reduces to $|k_d| \geq ||d_w + \tilde{\tau}||_\infty$.

# 7. TERMINAL-CONFIGURATION CONTROL WITH SENSOR/ACTUATOR NOISE COMPENSATION

Since linear controllability can be achieved with fewer actuators than nonlinear controllability, the robot designer can program actuators to switch from full actuation mode to a partial actuation mode, once the robot becomes sufficiently close to the final destination of its prescribed path. Once the unnecessary redundant actuators are "locked-up and turn-off", a significant amount of control energy savings is also possible. In contrast to the tracking control problem where robustness to feedback linearization errors is critical, in the regulation problem, robustness to sensor/actuator noise is investigated.

**Linear control problem statement.** Minimize the control energy in the presence of sensor and actuator noise subject to an output covariance bound. That is, for the linearized plant,

$$
\begin{aligned}
\dot{x} &= Ax + B_u u + B_w w \\
z &= C_z x \\
y &= C_y x + v
\end{aligned}
$$

in the presence of actuator noise $w$, and sensor noise $v$, we determine $A_c$, $B_c$, $C_c$ for the dynamic controller,

$$
\begin{aligned}
\dot{x}_c &= A_c x_c + B_c y \\
u &= C_c x_c
\end{aligned}
$$

that minimize $\lim_{t \to \infty} E(u^T u)$ subject to $\lim_{t \to \infty} E(zz^T) < \Omega$. It is assumed that $w$ and $v$ are zero-mean white noise processes with intensities $W$ and $V$, respectively. This optimization problem is convex and can be written

as a standard Linear Matrix Inequality (LMI) [17]:

$$\min_{U,K,X,Y} \operatorname{tr}(U) \quad \text{s.t.}$$

$$C_z X C_z < \Omega, \qquad \begin{bmatrix} U & K & 0 \\ K^T & X & I \\ 0 & I & Y \end{bmatrix} > 0$$

$$\begin{bmatrix} AX + XA^T + B_u K + K^T B_u^T & B_w \\ B_w^T & -W^{-1} \end{bmatrix} < 0, \qquad \begin{bmatrix} YA + A^T Y - C_y^T V^{-1} C_y & Y B_w \\ B_w^T Y & -W^{-1} \end{bmatrix} < 0$$

The controller becomes $A_c = A + B_u C_c - B_c C_y - Y^{-1}\Phi(I - XY)^{-1}$, $B_c = Y^{-1}C_y^T$ and $C_c = K(X - Y^{-1})^{-1}$ where $\Phi = YA + A^T Y + Y B B^T Y + C_y^T V^{-1} C_y$.

The plant matrices, $A$, $B_u$ and $B_w$, can easily be computed from the linearized model derived in the next section. In the last section, this controller is computed for a sequence of simple tensegrity robots to study the relationship between structural complexity and control effort.

## 8. TENSEGRITY MODEL

In [12], dynamic models of the form $M(q)\ddot{q} + V(q,\dot{q})\dot{q} + g(q) = H(q)f$ were developed for a class of tendon-driven robots that includes tensegrity structures. In this section, we give a concise summary of the results.
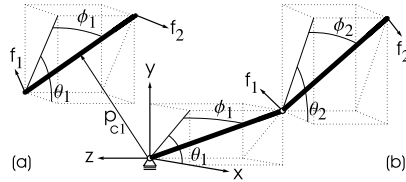


**Figure 5**. (a) Free-link. (b) Serial-link.

**Serial-link model.** The geometry of a serial-link rigid-body system with $b$ bars (links) is shown in Fig. (5b) for the two-bar case. Its $n$ degrees of freedom are organized as $q = \begin{bmatrix} q_1^T & q_2^T & \cdots & q_b^T \end{bmatrix}^T \in R^n$ where $q_i = \begin{bmatrix} \theta_i & \phi_i \end{bmatrix}^T$. The position of the $i^{th}$ bar's tip, $p_i$, is expressed as $p_i = p_o + \sum_{k=1}^{i} a_k \beta_k$ where $\beta_i = \begin{bmatrix} c\theta_i c\phi_i & s\theta_i c\phi_i & -s\phi_i \end{bmatrix}^T$, $c(\cdot) = \cos(\cdot)$, $s(\cdot) = \sin(\cdot)$, $a_i$ is the length of the $i^{th}$ bar. To construct the mass matrix we define $(3 \times n)$ matrices, $\Psi_i(q) = \begin{bmatrix} J_1 & J_2 & \cdots & J_i & O_{ni} \end{bmatrix}$ and $\Psi_{ci}(q) = \begin{bmatrix} J_1 & J_2 & \cdots & J_{i-1} & J_{ci} & O_{ni} \end{bmatrix}$, which consist of Jacobians, $J_i = a_i \partial \beta_i / \partial q_i$ and $J_{ci} = a_{ci} \partial \beta_i / \partial q_i$ and a matrix of zeros with $n - 2i$ columns, $O_{ni}$, where $a_{ci}$ as the distance from node to center of mass. $M \in R^{n \times n}$, $H \in R^{n \times 3b}$ and $g \in R^n$ become

$$M(q) = \mathcal{I}(q) + \sum_{i=1}^{b} m_i \Psi_{ci}^T(q) \Psi_{ci}(q), \qquad H(q) = \begin{bmatrix} \Psi_1^T & \Psi_2^T & \cdots & \Psi_b^T \end{bmatrix}, \qquad g(q) = \sum_{i=1}^{b} \Psi_{ci}^T f_{gi}$$

where $\mathcal{I} = \operatorname{diag}\begin{bmatrix} \mathcal{I}_1 & \mathcal{I}_2 & \cdots & \mathcal{I}_b \end{bmatrix} \in R^{n \times n}$, consists of inertial blocks, $\mathcal{I}_i = \operatorname{diag}\begin{bmatrix} \frac{m_i}{12}(a_i c\phi_i)^2 & \frac{m_i}{12}a_i^2 \end{bmatrix}$. Nodal forces, $f = \begin{bmatrix} f_1^T & f_2^T & \cdots & f_b^T \end{bmatrix}^T$, in cartesian space, $f_i \in R^3$, are induced by the tendon actuation system. If we denote the mass and coriolis/centripetal matrices elementwise as $M = [\mu_{kj}]$ and $V = [\zeta_{kj}]$, then $V(q,\dot{q})$ can be completely determined from $M(q)$ by using the following Christoffel parameters [2],

$$\zeta_{kj} = \frac{1}{2} \sum_{i=1}^{n} \left( \frac{\partial \mu_{kj}}{\partial q_i} + \frac{\partial \mu_{ki}}{\partial q_j} - \frac{\partial \mu_{ij}}{\partial q_k} \right) \dot{q}_i \tag{6}$$

**Free-link model.** For tensegrity structures designed with inertially-isolated rigid bars as depicted in Fig. (5a), a single bar has five degrees of freedom–three translations of its mass center, $p_{c1} \in R^3$, and two Euler angles,

$q_1 \in R^2$. Matrices $M \in R^{5 \times 5}$, $H \in R^{5 \times 6}$ and $g \in R^5$ are shown below. Use (6) again to get $V(q, \dot{q})$ from $M(q)$.

$$M(q) = \begin{bmatrix} m_1 I & 0 \\ 0 & \mathcal{I}_1(q_1) \end{bmatrix}, \qquad H(q) = \begin{bmatrix} I & I \\ -J_{c1}^T & J_{c1}^T \end{bmatrix}, \qquad g(q) = \begin{bmatrix} I \\ 0 \end{bmatrix} f_{g1}$$

**Global model.** Multiple copies of the serial-link and/or free-link model can be combined to create the global model of the entire robot structure. For instance, if we distinguish two non-contacting free-link models with subscript 1 and 2, the combined model becomes $M(q)\ddot{q} + V(q, \dot{q})\dot{q} + g(q) = H(q)f$ where $M = \text{diag}[M_1, M_2]$, $V = \text{diag}[V_1, V_2]$, $H = \text{diag}[H_1, H_2]$ and $q = [q_1^T, q_2^T]^T$ and $f = [f_1^T, f_2^T]^T$. Given an $m$-tendon network, the tendon orientation vectors, $\ell$, are defined in terms of the nodal points, $p$, as $\ell = Cp$. Examples that illustrate how to build this network are given in [12]. The direction cosine matrix becomes $D = \text{diag}[d_1, d_2, \ldots, d_m]$, where $d_i = \ell_i (\ell_i^T \ell_i)^{-1/2}$. The principle of virtual work yields $f = C^T D t$, where $t \in R^m$ is the vector of tendon forces. If we define $G := HC^T D$, the rigid-body and tendon-actuation systems can be joined to yield the global model,

$$M(q)\ddot{q} + V(q, \dot{q})\dot{q} + g(q) = G(q)t$$

**Linearized model.** In linear control modes such as precision regulation, it is advantageous to work with a linearized model. If we assume the tendon forces obey Hooke's Law, $t = S(\ell(q) - u)$ where $S$ is a diagonal matrix of spring constants, $\ell(q)$ is the stretched tendon length and $u$ is the unstretched tendon length, then linearizing the global model about the static operating point, $(\bar{q}, \bar{u})$ yields

$$\tilde{M}\ddot{\tilde{q}} + \tilde{D}\dot{\tilde{q}} + \tilde{K}\tilde{q} = \tilde{B}\tilde{u} \tag{7}$$

where $\tilde{u} = u - \bar{u}$, $\tilde{q} = q - \bar{q}$, $\dot{\tilde{q}} = \dot{q}$, $\ddot{\tilde{q}} = \ddot{q}$, $\tilde{M} = M(\bar{q})$, $\tilde{D} = 0$, $\tilde{B} = -G(\bar{q})S$ and the stiffness matrix becomes

$$\tilde{K} = \left.\frac{\partial g(q)}{\partial q}\right|_{\bar{q}} - G(\bar{q})S \left.\frac{\partial \ell(q)}{\partial q}\right|_{\bar{q}} - \sum_{k=1}^{n_u} \left.\frac{\partial G(q)S(:,k)}{\partial q}\right|_{\bar{q}} (\ell_k(\bar{q}) - \bar{u}_k)$$

## 9. OPTIMIZING STRUCTURE/CONTROL USING SELF-SIMILAR APPROACH

It is possible to reduce system mass by introducing more stages to the tensegrity structure, while keeping the total length constant. However, adding additional stages (and thus additional noisy actuators) potentially increases the noise effect which can compromise tracking precision. Hence, the optimal number of stages can be viewed as a tradeoff between maximizing precision and minimizing system mass. The simple example of figure (6b) illustrates the design process to determine the optimal number of stages of a tensegrity robot.
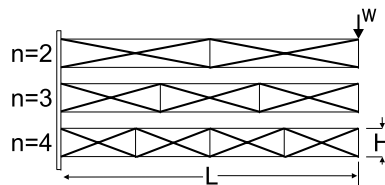


**Figure 6**. Stage replication subject to a fixed external geometry

**Self-similar concept and minimum mass.** The self-similar concept can be used to answer the question, "How many stages will lead to a minimum mass, while sustaining a specified level of pretension?". In this problem, the limiting factor in mass minimization comes from the buckling of the bars, and the failure of the tendons. The bars and tendon diameters are chosen such that all structural members fail simultaneously, for the

prescribed pretension level (tension $F$ in the horizontal tendons). The buckling load of a cylindrical tube with outer radius, $r$, and inner radius, $r_i = \beta r$, is expressed by:

$$F_{buckling} = \frac{\pi^3 E r^4}{4L_b^2}(1 - \beta^4)$$

(8)

where $E$ is the material Young's modulus, $r$ is the cross section radius and $L_b$ is the length of the bar. Regarding the tendons, the maximum tensile load is given by:

$$F_{yield} = \sigma_y S$$

(9)

where $\sigma_y$ is the *yield stress* of the tendon, and $S$ its cross sectional area. Using (8) and (9) together with a simple derivation of the forces in every member of the structure, one can compute the total mass (yielding general failure for pretension $F$), as a function of the number of stages $n$: $M_{total} = M_{bars} + M_{tendons}$ where

$$M_{bars} = \frac{4\rho_b}{n}\sqrt{\frac{F(1-\beta^2)}{\pi EL(1+\beta^2)}}(n^2 H^2 + L^2)^{5/4}, \qquad M_{tendons} = \frac{2\rho_s F H^2}{\sigma_y L}n(n-1/2) + \frac{2\rho_s L F}{\sigma_y}$$

(10)

If we assume $M_{tendons} \ll M_{bars}$, first and second derivative tests of $M_{bars}(n)$ yields an analytical solution for the number of stages to use for the minimum mass structure,

$$\min_n M_{bars}(n) \quad \Longrightarrow \quad n^* = \frac{L}{H}\sqrt{\frac{2}{3}}$$

where $n^*$ is then rounded to the nearest integer. Figure (7a) shows the evolution of the total mass (in $kg$) of the
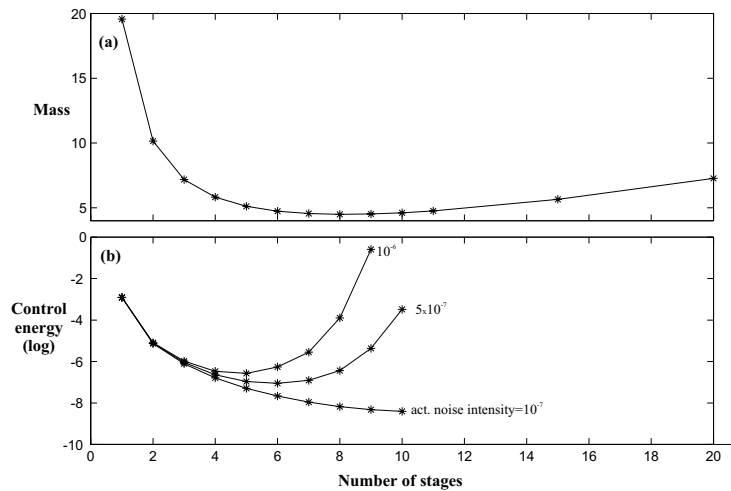


**Figure 7.** Self-similar structure concept: (a) evolution of mass with increasing number of stages (b) evolution of control energy with increasing number of stages

structure of figure (6b) in terms of the number of stages (number of self-similar iterations). For this particular example, $L = 10m$, $H = 1m$, the bars are made of steel (Young's modulus,$2.1 \cdot 10^{11} N/m^2$; density,$7850 kg/m^3$), the tendons are made of carbon (Young's modulus, $2.3 \cdot 10^{11} N/m^2$; density,$1750 kg/m^3$; $\sigma_y = 3.5 \ 10^8 N/m^2$), and the structure is designed to support a pretension $F = 50N$ (refer to figure (6) for notations). The mass of the tendons represents only 0.5% of the total mass for $n = 20$. In our example, the 8-stage configuration leads to the minimum mass, whereas the number of stages leading minimal control energy varies with the actuator/sensor quality, as we discuss below.

**Self-similar concept and minimum control energy.** The self-similar concept can be used to answer the question, "How many stages will lead to a minimum control energy, while sustaining a specified level of pretension?". As will be discussed shortly, the limiting factor in the control energy minimization is the signal-to-noise ratio of the control tendons. Previously, we discussed how the mass of the structure can be decreased while keeping the same static resistance to a constant axial load $F$ (or equivalently keeping the same pretension $F$). In what follows, we add some external random noise disturbance (mean zero, intensity $10N^2$) acting vertically on the tip of the structure, and we would like to keep the position of the tip within some admissible range ($10^{-2}m$ standard deviation). The overall configuration is represented in figure (8). The structure is controlled
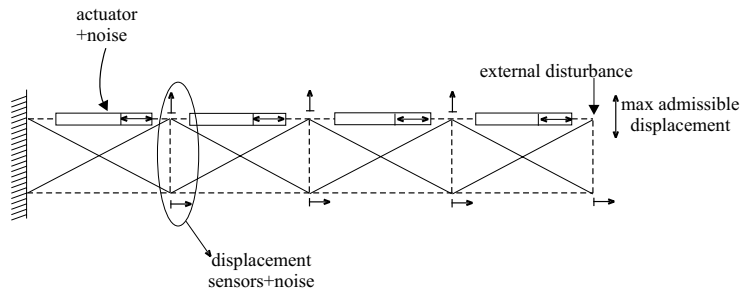


**Figure 8**. control simulation configuration

by linear-displacement actuators changing the rest length of the top horizontal strings. Displacement sensors are located at every node. Both sensors and actuators are noisy (actuator noise is given in figure (7b), and sensor noise intensity is always $10^{-7}m^2$ for every sensor.) We designed a controller to minimize the control energy (variance), subject to the constraint: tip displacement has a standard deviation less than $10^{-2}m$. This calculation has been repeated for increasing number of stages. Results are displayed in figure (7b). The three curves correspond to three different levels of actuator noise. Some general remarks can be formulated from this example: (i) there exists an optimum number of stages leading to the minimum control energy (ii) less noisy the actuators lead to more stages (thus actuators) for minimum control energy, (iii) the minimum control energy decreases when actuator noise decreases. (iv) The 8-stage plant has minimum mass and minimum control energy when the actuator noise intensity is $2 \times 10^{-7}m^2$. Hence, it is possible to construct tensegrity structures that are minimum mass and require minimum control energy during precision regulation of the robot in its terminal configuration.

## 10. CONCLUSION

This paper describes a feedback linearization control law that uses the parameters in the nullspace of the control distribution matrix, $G$, to minimize the norm of the tendon force tracking error, $\|t - t_d\|$, while avoiding saturation of the control signals. In addition to saturation avoidance, we have shown these free parameters can also be designed for minimum force control using a constrained infinity norm minimization. Control techniques for point-to-point maneuvering along a prescribed path in minimum time have also been extended to include the case where multiple kinematically-invertable units undergo independent reconfigurations. During the post-movement phase of a point-to-point maneuver, linear control simulations are used to select the number of tensegrity stages and the actuator precision such that the expended control energy and structural mass are jointly minimized. Future work will focus on smoothing control laws and jointly optimizing the tendon and rigid-link topologies for specific applications, such as delicate-object handling and locomotion in constricted environments.

## REFERENCES

1. H. Asada and J.-J. E. Slotine, *Robot Analysis and Control*, Wiley, 1986.
2. M. Spong and M. Vidyasagar, *Robot Dynamics and Control*, Wiley, 1989.
3. F. Lewis, C. Abdallah, and D. Dawson, *Control of Robotic Manipulators*, Macmillian, 1993.

4. D. Deno, R. Murray, K. Pister, and S. Sastry, "Fingerlike biomechanical robots," in *Proceedings of the IEEE International Conference on Robotics and Automation*, 1992.

5. C. Johnstun and C. Smith, "Modelling and design of a mechanical tendon actuation system," *ASME Transactions Journal on dynamics, system, measurements and control* , 1992.

6. W. Townsend and J. Guertin, "Teleoperator slave - w.a.m. design methodology," *Industrial Robot* **26**(3), pp. 167–177, 1999.

7. V. Hayward and J. Cruz-Hernandez, "Parameter sensitivity analysis for design and control of tendon transmission," in *Experimental Robotics*, Lecture Notes in Control and Information Sciences, (London), 1995.

8. R. Skelton, J. Helton, R. Adhikari, J. Pinaud, and W. Chan, "An introduction to the mechanics of tensegrity structures," in *Conference on Decision and Control*, **5**(5), pp. 4254–9, 2001.

9. R. Murray, Z. Li, and S. Sastry, *A Mathematical Introduction to Robotic Manipulation*, CRC Press, 1994.

10. A. Bicchi and D. Prattichizzo, "Analysis and optimization of tendinous actuation for biomorphically designed robotic systems," *Robotic systems* , 2000-1.

11. H. Kobayashi, K. Hyodo, and D. Ogane, "On intellegent control of tendon-driven robotic mechanisms with redundant tendons," *International Journal of Robotics Research* **17**(5), pp. 561–571, 1998.

12. J. Aldrich, R. Skelton, and K. Kreutz-Delgado, "Control synthesis for a class of light and agile robotic tensegrity structures," in *American Control Conference*, 2003.

13. J. Bobrow, S. Dubowsky, and J. Gibson, "Time-optimal control of robotic manipulators along specified paths," *The International Journal of Robotics Research* **4**(3), 1985.

14. M. do Carmo, *Differential Geometry of Curves and Surfaces*, Prentice Hall, 1976.

15. J.-J. E. Slotine and H. Yang, "Improving the efficiency of time-optimal path-following algorithms," *IEEE Transactions on Robotics and Automation* **5**(1), pp. 118–124, 1989.

16. Z. Qu and D. Dawson, *Robust Tracking Control of Robot Manipulators*, IEEE Press, 1996.

17. R. Skelton, T. Iwasaki, and K. Grigoriadis, *A Unified Algebraic Approach to Linear Control Design*, Taylor and Francis, 1998.